Environmental Science: Atmospheres

ROYAL SOCIETY OF CHEMISTRY

PAPER

View Article Online
View Journal | View Issue

Check for updates

Cite this: *Environ. Sci.: Atmos.*, 2025, **5**, 316

Emissions from agricultural fires in India: field measurements of climate relevant aerosol chemical and optical properties†

Taveen Singh Kapoor, [ae] Gupta Anurag,[ab] Chimurkar Navinya, [a] Saurabh Lonkar,[b] Kajal Yadav,[c] Ramya Sunder Raman, [c] Chandra Venkataraman [ad] and Harish C. Phuleria *[ab]

Carbonaceous aerosol particles are associated with large uncertainties in their climate impacts because of incomplete knowledge of their optical properties and emission magnitudes. Biomass-burning sources significantly contribute to carbonaceous aerosol emissions in India, with crop residue burning being crucial during post-harvest months. Here, for the first time, we study the chemical and optical properties of emission aerosols using *in situ* real-time and filter-based measurements from significantly contributing crop residue straws, stalks, and stems in India. Emitted particles exhibited optical behaviour characteristic of the brown-black carbon absorption continuum, with large mass absorption cross-sections (MAC_{520}: 8.2 ± 9.6 m^2 g^{-1}) and small absorption Angström exponents ($AAE_{370/660}$: 1.97 ± 0.81). They contain significant amounts of lower volatility organic (OC_{LV}) and elemental carbon fractions. The relative abundances of OC_{LV} correlate positively with MAC_{520} and negatively with $AAE_{370/660}$, implying significant absorption exerted by OC_{LV}, with likely atmospheric persistence. Additionally, we measured emission factors for a complete list of particulate chemical constituents. Emission factors of elemental carbon are larger than those in earlier studies, indicating a 1.6–3.8 times increase in the climate warming potential of the emitted particles from crop residue burning. The intrinsic property measurements and the emissions estimates made here can aid climate modelling efforts that underestimate aerosol absorption in the region.

Received 26th July 2024
Accepted 4th November 2024

DOI: 10.1039/d4ea00104d

rsc.li/esatmospheres

Environmental significance

Agricultural residue fires are significant sources of atmospheric aerosols in South Asia, contributing to severe air quality episodes in the region. However, their climate impacts remain highly uncertain. Here, we made *in situ* emission measurements of prescribed agricultural fires in India to study aerosol chemical and optical properties and examine their interrelationships. The measurements were used to prepare source profiles and calculate emission factors and emission magnitudes from this source over India. This is an improvement on previous emissions inventories that rely on emission factors from other world regions that may not be representative of emissions in South Asia. Our findings show a substantial increase in absorbing species that can drive improvements in regional and global climate models that underestimate aerosol absorption.

1 Introduction

Carbonaceous aerosols are key short-lived climate forcers (SLCFs), whose mitigation is critical to achieving global 1.5° and 2° temperature targets[1,2] and other air quality co-benefits.[3] However, estimates of radiative impacts continue to suffer from large uncertainties.[4,5] One source of uncertainty stems from a limited understanding of aerosol emissions, including their magnitudes and chemical and optical properties.[5–7] The Indian National Carbonaceous Aerosols Programme (NCAP)-Carbonaceous Aerosol Emissions, Source Apportionment and Climate Impacts (COALESCE) network[8] targets the study of major biomass-burning aerosol emissions sources, including residential cooking[9] and heating,[10] clay-fired brick production,[11]

[a]*Centre for Climate Studies, Indian Institute of Technology Bombay, Mumbai 400076, India. E-mail: phuleria@iitb.ac.in*

[b]*Environmental Science and Engineering Department, Indian Institute of Technology Bombay, Mumbai 400076, India*

[c]*Department of Earth and Environmental Sciences, Indian Institute of Science Education and Research Bhopal, Bhopal 462066, India*

[d]*Department of Chemical Engineering, Indian Institute of Technology Bombay, Mumbai 400076, India*

[e]*Department of Energy, Environmental and Chemical Engineering, Washington University in St. Louis, St. Louis 63130, USA*

† Electronic supplementary information (ESI) available: Measured pollutant concentrations, uncertainty calculations, estimated crop- and state-specific emissions, and comparisons with the literature. See DOI: https://doi.org/10.1039/d4ea00104d

and agricultural residue burning.[12] Agricultural residue burning is among the significant contributors to SLCF emissions globally, especially in the south and southeast Asian regions.[13–15] In India, crop residue burning emissions are especially relevant during short periods post-harvest, contributing to poor ambient air-quality episodes.[16–18]

Emissions from crop residue burning are calculated by multiplying the activity with emission factors. Activity is the quantity of crop residue burned on-field, calculated using top-down[19,20] or bottom-up[13,14,21,22] approaches. Meanwhile, the emission factors, or the amount of pollutant emitted per unit mass of crop residue burned, are calculated using lab-simulated,[23–31] *in situ* (field),[32–38] or aircraft (field)[39] measurements. Lab-simulated measurements provide ease and flexibility but cannot mimic field combustion conditions (*e.g.* the fuel equivalence ratio and meteorology) and fuel properties (*e.g.* moisture).[15,39–41] Considering the above, field measurements give more accurate emission factor estimates. Several types of crop residues are burned on-field, including cereals, sugarcane, oilseeds, and fiber crops.[12,42] They have varying elemental compositions, are harvested and burned on-field in different seasons and likely have different emission properties.

Crop residue aerosol emissions comprise inorganic and organic species that absorb and scatter solar radiation. Amongst these, black carbon (BC) particles are the strongest absorbing species with a weak absorption wavelength dependence.[43] Along with BC, absorbing organic carbon species called brown carbon (BrC) are also emitted.[44] BrC particles exhibit relatively weaker absorption strengths but a higher absorption wavelength dependence.[45] The presence of a wide variety of organic carbon species in the atmosphere leads to large variations in their optical properties. Saleh *et al.*[46] proposed a light-absorption continuum from weakly absorbing brown to strongly absorbing black carbon with increasing absorption strengths, where absorption strength is inversely proportional to its wavelength dependence. Particles with stronger absorption strengths likely have lower volatility, larger molecular weights, and lower water solubility. Low-volatility particles are found in lab-based combustion of hydrocarbon[46,47] and biomass[48,49] and also in field-measured wildfire[50,51] and anthropogenic[52,53] emissions. However, these particles are difficult to detect using commonly used solvent extraction techniques because of their insolubility.

Absorption properties of atmospheric carbonaceous aerosols, especially those influenced by crop residue biomass burning, have been reported in the literature[54–62] and are essential to validate and constrain climate model simulations. However, the model simulations remain strongly dependent on the emission characteristics at the source. Despite significant emissions from crop residue burning in the south-Asia region, only two studies[37,38] have reported field measurements of crop residue burning in the region. The paucity of data, both the number of measurements and types of crops, limits global emissions inventories to using broad crop-averaged emission factors measured across the world to estimate emissions from India.[63–65] Some regional inventories have used crop (or crop-group) specific emission factors,[13,66] but using measurements made in other regions of the world that may not be representative of the south-Asian region for the reasons already discussed.

Here, we study the physicochemical and optical properties of aerosol emissions from crop residue burning in western India using *in situ* field measurements. The measurements include real-time aerosol optical properties and time-integrated, filter-based chemical speciation to estimate emission factors. Relationships between chemical component concentrations and optical properties are also reported, suggesting that the brown-black absorption continuum exists in real-world prescribed biomass burning emissions. Furthermore, the emission factors are combined with activity estimates from a previous study to produce high spatiotemporal resolution climate model-ready emission estimates.

2 Methodology

2.1 Measurement location

Previous studies have reported burning residues of rice, wheat, sugarcane, other cereals, and oilseeds in India.[12,13,22,42] In the present study, we report emission measurements from burning agricultural residues, including wheat (straw), cotton (stalks), oilseeds (stalks), and banana (stems and leaves) biomass, which constitute 78% of the crop residue biomass burned on-field in western India and 45% in India.[12] Field emission measurements of these crops were made in five villages in Vadodara and Anand districts in Gujarat, India (Fig. S1†). Farmers were contacted before the harvest seasons to gather information on dates of residue-burning activities; field measurements were conducted during these periods. 3–8 emission measurements of each crop residue type were made to ensure repeatability and establish confidence in the results. Where possible, emissions from the same crops in different villages were measured to capture possible heterogeneity in emission properties.

Measurements were conducted during the rabi harvest season (March and April) of 2022, with additional measurements of banana residue burns during the kharif harvest season (October–November) of 2021. Measurements were conducted in fields away from other emission sources to ensure minimal interference. The farms were away from major roads, with traffic emissions, and village centres, with residential biomass burning emissions from cooking, water heating and space heating. On the day of the burn on a field, the sampling system was set up before the burn to briefly record the background concentrations and confirm the absence of interference from other sources. Aerosol sampling on filter substrates was started as soon as the fire was ignited, and aerosols were sampled until the smouldering combustion died down. This ensured that the sampling was representative of the entire combustion cycle and real-world meteorological conditions. The measurement campaigns lasted 2–3 weeks, including two background measurements during each campaign, once in the middle of the campaign and another at the end. Background aerosols were measured for 8–10 hours to ensure sufficient particle concentrations on filter substrates for subsequent chemical analyses. These background measurements were also conducted in

agricultural fields away from other aerosol sources when no field was burning nearby. The measured background concentrations were used to calculate elevations in concentrations of all the species during the burns, which are required for emission factor calculations. For all the species apart from CO_2, the background concentrations had <5% of the smoke plume concentrations (Table S1†).

2.2 Measurement method

The measurements were conducted using the versatile source sampling system (VS3), specifically designed to study aerosol emissions from biomass burning sources for the COALESCE network.[8] VS3 is described in detail elsewhere[67] and is inspired by other portable source emissions systems.[68,69] Briefly, it consists of a multi-arm inlet (adapted from Roden *et al.*[68]) with eight arms that aspirated aerosols iso-kinetically in a mixing plenum. The orientation of the multi-arm inlet was modified depending on the type of fire and wind conditions; this is discussed in detail in Section 2.2.1. The aspirated aerosols were then divided into gaseous and particle sampling lines to measure gaseous and aerosol particle concentrations and optical properties. The particle sampling line consisted of real-time instruments to measure optical properties and a filter-sampling system to collect particles on filter substrates for chemical analyses. In the gas sampling line, concentrations of CO_2 and CO were measured using gas analysers (TESTO 350 and TESTO 480 IAQ Analyser; Testo SE & Co. KGaA, Germany). Elevations in the concentrations of CO_2 (ΔCO_2) and CO (ΔCO) above the background were used to estimate the modified combustion efficiency (eqn (1)), a commonly used measure shown to influence carbonaceous aerosol emission properties.[48,70,71] Other gases, SO_2 and NO_x, were also measured, but their concentrations were below the instrument detection limits. In the particulate sampling line, aerosol particles were simultaneously collected on polytetrafluoroethylene or PTFE, nylon, and quartz filter substrates using an aerosol multi-stream sampler (URG, USA). Also in the particulate line were real-time instruments measuring aerosol absorption using an aethalometer (AE33, Magee Scientific, USA), which uses a dual-spot algorithm to make filter-substrate corrections.[72] Scattering coefficients were measured using an integrating nephelometer (IN102, AirPhoton, USA) employing manufacturer-recommended correction factors.[73] The real-time particle measurement instruments were placed downstream of a dilution plenum to ensure that the aerosol concentrations were within the measurable limits of the instruments.

$$\mathrm{MCE} = \frac{\Delta CO_2}{\Delta CO_2 + \Delta CO} \quad (1)$$

The aerosol particles collected on filter substrates were subjected to lab analyses using standard COALESCE network[8] protocols.[74–76] PTFE filters were used to estimate gravimetric $PM_{2.5}$. The filters were pre- and post-weighed using a microbalance (Sartorius Cubis MSU 6.6S) with the least count of 1 μg (range 11 μg to 2.1 g). Before being weighed, the PTFE filter substrates were pre-conditioned at 25 °C and 50% RH. After gravimetric $PM_{2.5}$ measurements, the loaded PTFE filters were used to determine elemental concentrations using X-ray fluorescence (XRF) spectrometry (SPECTRO X-LAB 2000, SPECTRO Analytical Instruments, Germany).[74] The nylon filters were used to measure water-soluble inorganic ions using ion chromatography (Dionex ICS-1100, Thermo Fisher Scientific, USA).[75] Quartz filters were used to measure elemental and organic carbon concentrations using thermo-optical analysis (DRI 2015 total carbon analyzer, Desert Research Institute, USA) using the IMPROVE_A TOR protocol.[76,77] The measured EC (thermo-optically defined) concentrations are treated equivalent to BC (optically defined) concentrations throughout the manuscript. While both EC and BC are fundamentally graphite-like soot particles exhibiting strong absorption and refractory properties, they have different operational definitions[43] but are used interchangeably in emissions estimates.[15]

The measured quantities were used to calculate the intrinsic aerosol properties of the emitted aerosol. The real-time multi-wavelength (λ) absorption coefficients ($b_{abs,\lambda}$) were used to calculate the absorption Angström exponent (eqn (2), $AAE_{\lambda_1/\lambda_2}$), a measure of the wavelength dependence of absorption. $AAE_{370/660}$ is influenced by both black and brown carbon absorption; meanwhile, $AAE_{660/880}$ is likely dominated by black carbon absorption. The absorption and scattering ($b_{scat,\lambda}$) coefficients were also used to calculate the single scatter-albedo (SSA, eqn (3)), a measure of the aerosol's relative absorption or scattering nature. The experiment averaged absorption coefficients are divided by the $PM_{2.5}$ to calculate the mass absorption cross section (MAC, $m^2\ g^{-1}$, eqn (4)), a measure of aerosol absorption strength. MAC and SSA are reported at 520 nm, the wavelength at which incident solar radiation has the peak energy that is absorbed by the emitted particles.

$$\mathrm{AAE}_{\lambda_1/\lambda_2} = -\frac{\log\left(\frac{b_{abs,\lambda_1}}{b_{abs,\lambda_2}}\right)}{\log\left(\frac{\lambda_1}{\lambda_2}\right)} \quad (2)$$

$$\mathrm{SSA}_\lambda = \frac{b_{scat,\lambda}}{b_{scat,\lambda} + b_{abs,\lambda}} \quad (3)$$

$$\mathrm{MAC}_\lambda = \frac{b_{abs,\lambda}}{PM_{2.5}} \quad (4)$$

The organic carbon thermal carbon fractions (OC1–OC4) were estimated by measuring CO_2 emitted at various temperatures using the total carbon analyser. The volatility of organic carbon (OC) released at different temperatures is inversely proportional to temperature; higher temperatures result in less volatile OC fractions.[78,79] Here, we divide the organic carbon thermal fractions into higher volatility OC (OC_{HV}), the sum of OC1 and OC2 (emitted at 180 °C and 280 °C, respectively) and lower volatility OC (OC_{LV}), the sum of OC3 and OC4 (emitted at 480 °C and 580 °C, respectively) to study their variation with combustion conditions and optical properties.

$$\frac{OC_{HV}}{OC_{LV}} = \frac{OC1 + OC2}{OC3 + OC4} \quad (5)$$

2.2.1 Inlet configurations. Previous studies conducting *in situ* emission measurements of agricultural residue burning have used a single static tube inlet or grab sampled emission plumes downwind of the emission plume at heights ranging from 1–3 m.[33,34,38] In this study, we use a multi-arm inlet to capture emissions plumes over a larger area and avoid loss of sampling time that may arise from changes in wind directions when using a single tube inlet. The multi-arm inlet was mounted on a stand at a height varying from 1.5–2.5 m, depending upon the burning configuration, to allow for some natural dilution. The configuration of the arms was based on the type of residue and the harvest mechanism.

Crop-residues are burned on the field in two configurations across the world.[32–35,37,38] The first is a spread on-field *in situ* configuration where the residues are left on-field after harvesting by hand or using combine harvesters. Combine harvesters are machines that harvest and thresh crops in a single operation, and the residue left behind on the field is especially difficult to handle for farmers. Wheat and rice residues are generally burned on-field in this manner; the field is set alight from one side of the field, and the wind facilitates propagation of the fire across the field. Since the emitted plume advects at an angle with the ground (not vertically), the multi-arm inlet was kept vertical (Fig. 1c). In some cases, when the pollutant concentrations were not elevated enough for detection using the instruments, the fire was chased across the field (Fig. 1d) such that the inlet was closer to the fire front. Stalks and stems and leaves residues, meanwhile, are made into several piles on-field after harvest and set alight in batches. When the residue is piled on-field, the plume may advect vertically, and the inlet was kept horizontal (Fig. 1b). The plume may also advect horizontally when winds are stronger, and the multi-arm was kept vertical in these situations (Fig. 1a). Agricultural residue burns typically last from 10 minutes to a couple of hours, depending on field (spread configuration) or pile size (piled configuration). To ensure sufficient data for real-time instruments without overloading the filter substrates, we measured emissions for fires that lasted 10–20 minutes.

2.3 Calculating emission factors

The carbon balance method[68,80] was used to calculate emission factors. It relies on the estimation of emitted species that contain carbon (CO_2, CO, CH_4 BC, OC, and hydrocarbons), which act as a proxy for the quantity of the fuel or biomass burned. Carbon emissions from crop residue burning are primarily in CO_2 and CO, with the remaining species only contributing to about 3.5% of the emitted carbon mass.[15,63] Here, we only consider CO_2 and CO emissions in the carbon balance equation and neglect the other species, a commonly employed simplification when using this method.[33,34,36,68] The method (eqn (6)) uses a ratio of the increase above ambient levels in the pollutant species' concentration ($[\Delta X]$, μg m^{-3}) relative to that of CO_2 (ΔCO_2) and CO (ΔCO). Therefore, the carbon balance presents an advantage of flexible natural dilution, as it relies on the ratios of changes in concentrations of the

Fig. 1 Photographs of crop residue burning emission measurements showing different configurations of the multi-arm inlet: (A) piled residue with vertical advection of plume, (B) piled residue with horizontal advection of wind, (C) spread residue with a static inlet with vertical configuration, and (D) spread residue with a moving multi-arm inlet.

pollutants and not the absolute concentrations. The carbon balance method also requires other parameters to calculate emission factors, including the carbon density per unit volume of CO/CO_2 (ρ_{C,CO_2}, $kg_C\ m_{CO_2}^{-3}$), calculated using real-time measurements of the temperature of the emission plume and ideal gas equations. The carbon fraction was calculated using the ultimate analysis (Thermo Finnigan Flash EA1112 series CHNS analyser) of crop residue samples taken from the field (ESI Section S1†). Emission factors of crop residues were distributed into three major groups: straws (wheat), stalks (cotton and oilseed), and stems and leaves (banana). In general, straws have lower density and are fired when spread on-field; meanwhile, stalks have a higher density and are burned in piles.

$$EF_X = [\Delta X] \times \frac{1}{\Delta CO_2 + \Delta CO} \times \frac{1}{\rho_{C,CO_2}} \times CF \quad (6)$$

The carbon balance method is dependent on elevations in the concentrations of CO_2 and CO to estimate emission factors, and a larger increase above the background is desirable for accurate emission factor estimates. Placing the inlet close to the fire would increase the CO_2 concentrations; however, it may not allow for natural dilution of the emissions plume. Natural dilution is necessary for the initial atmospheric processing of the emitted aerosols so that the reported emission factors are ready for climate modelling applications. Therefore, the distance between the sampling inlet was balanced such that the aspirated aerosols were at nearly ambient temperatures while ensuring sufficient elevations in CO and, more importantly, CO_2. The delicateness of this task is demonstrated in Fig. S2,† which shows that concentrations of CO_2 reach values close to ambient levels when combustion reaches the smouldering phase. The lower concentrations of CO_2 (and particle matter absorption) towards the end of experiments also indicate minimal interference of the emission plume from other emission sources.

2.3.1 Uncertainty in emission factors. Uncertainty in emission factors of each experiment was calculated by taking the uncertainty in each term of the carbon balance equation (eqn (6)) and propagating it in quadrature. These calculations gave an overall relative uncertainty of 25%; details of the calculations are shown in ESI Section S4.† We report the emission factor for a crop type as the mean of all the measured values for the crop type; however, inter-experimental differences in combustion conditions and fuel composition can also influence emission factors. Propagating the uncertainties in individual experiments to the mean values for the crop type would retain the 25% relative uncertainty. We also calculated the uncertainty in terms of the emission factors' standard deviations, which were larger than the propagated uncertainties. Therefore, we report the conservatively greater uncertainties calculated as the standard deviation of the measurements throughout the manuscript for consistency. However, we recommend using the standard deviation of the mean or 25% of the calculated mean, whichever is larger, as the uncertainty value.

2.4 Emission calculations

District ('d')-, crop ('c')-, and pollutant ('p')-specific emissions ($EM_{d,c,p}$) were calculated (eqn (7)) using the crop-residue type (straws, stalks, and leaves and stems) specific emission factors ($EF_{c,p}$) from the present study. We would ideally like to use crop-specific emission factors, especially for crops burned in large amounts (such as rice and sugarcane). However, since such measurements are not available in the region, we use emission factors for similar crop types measured in the present study. Cereal crop emission factors were used for rice, wheat, maize, and millets; stalk emission factors for oilseeds, cotton, and sugarcane; and stems and leaves emission factors for banana residue burning. These emission factors present an improvement on previous emissions inventories that use crop-independent emission factors derived from studies in other regions of the world.

Estimates of district-wise activity ($activity_{d,c}$), or the mass of crop residue burned on-field, were taken from Kapoor *et al.*[12] They employed the bottom-up framework, commonly used to estimate emissions from crop residue burning.[13,14,21,66] Briefly, activity was calculated by multiplying five variables that may vary with the district ('d') and crop type ('c') (eqn (8)). The first variable is crop production ($PROD_{d,c}$), the data for which were taken from the Ministry of Agriculture and Farmers Welfare statistics.[81] Other variables include the crop residue produced per unit mass of crop production, or the residue-to-crop ratio (RCR_c), the fraction of dry matter by mass in the residue (or the dry-matter-fraction, DMF_c), and the fraction of dry residue contributing to emissions, *i.e.*, the mass excluding the ash content (or the fraction-actually-oxidized, FAO_c); crop-specific data for these terms are taken from previous literature.[21,82] The last variable for activity estimation and likely the most uncertain is the fraction of the generated residue subjected to on-field burning (or fraction burned, $FB_{d,c}$).

Fraction burned can have large spatial heterogeneity across the country, depending upon the types of crops and quantities of crops grown in the region and the uses the residues are put to, which may further be dependent upon socio-economic factors. Hence, to determine the fraction burned, over 2400 questionnaire surveys were conducted across villages in 43 districts of the country covering major crop-growing areas. Farmers were asked about the crops they grew and the fraction of the residue subjected to on-field burning. This information, collected for 43 districts, was extrapolated to all the country's districts using crop-specific multivariate regression models. The regression models were developed using the surveyed crop- and district-specific fraction burned values as the dependent variables to be predicted and socioeconomic, livestock, and satellite-retrieved active fire and land cover type information as independent variables. Socio-economic information was taken from the census of India statistics,[83] including population, economic, and education variables. Livestock information included the number of buffaloes, cattle, and pigs across the different districts.[84] Ultimately, the multivariate regression models gave district- and crop-specific fraction burned values for important crops burned across the country, a first country-wide attempt to estimate the parameter using primary, field-derived information.

$$\mathrm{EM_{d,c,p}} = \mathrm{activity_{d,c}} \times \mathrm{EF_{c,p}} \quad (7)$$

where

$$\mathrm{activity_{d,c}} = \mathrm{PROD_{d,c}} \times \mathrm{RCR_c} \times \mathrm{FB_{d,c}} \times \mathrm{DMF_c} \times \mathrm{FAO_c} \quad (8)$$

The activity data and, hence, the emissions are calculated at annual and sub-country (district) scales. For application to climate models, these need to be distributed spatially (grids) and temporally (days or months). Temporal ('t') distribution of emissions within a district ($\mathrm{EM_{t,d}}$) (eqn (9)) was done using the daily variability of fire counts in croplands in a district ($\mathrm{frac_{t,d}}$) (eqn (10)). These were calculated using a Moderate Resolution Imaging Spectroradiometer (MODIS) retrieved fire counts ($\mathrm{FC}_{t,x,y}$, MCD14A2 product, resolution: 0.01° × 0.01°)[85] weighted by the fraction of cropland area, taken from MODIS retrieved spatial distribution of croplands ($\mathrm{frac_{agri}}$, MCD12Q1 product, resolution: 0.05° × 0.05°)[86] across grids (denoted by x,y).

$$\mathrm{EM_{t,d}} = \mathrm{EM_d} \times \frac{\mathrm{frac_{t,d}}}{\sum_{\mathrm{t}} \mathrm{frac_{t,d}}} \quad (9)$$

where

$$\mathrm{frac_{t,d}} = \sum_{x,y \in \mathrm{d}} \left(\mathrm{FC}_{t,x,y} \times \mathrm{frac}_{\mathrm{agri},x,y}\right) \quad (10)$$

Furthermore, emissions within a district ($\mathrm{EM_{t,d}}$) were distributed to grids using MODIS land-cover-type information.[85] Each 0.05° × 0.05° grid within a district is assigned emissions proportional to the fraction of cropland it covers in the district (eqn (11)).

$$\mathrm{EM}_{x,y,\mathrm{t}} = \frac{\mathrm{frac}_{\mathrm{agri},x,y}}{\sum_{x,y \in \mathrm{d}} \mathrm{frac}_{\mathrm{agri},x,y}} \times \mathrm{EM_{t,d}} \quad (11)$$

3 Results and discussion

3.1 Calculated emission factors

The carbon balance method uses elevations in concentrations of pollutant species in emitted smoke above their ambient levels to calculate emission factors. CO_2 and CO elevations (97–667 ppm and 3–145 ppm, respectively, shown in Table S1†) were used to estimate emission factors of all the species; their respective emissions factors are in the range 1306–1389 g kg^{-1} and 74–97 g kg^{-1} (Table 1). Changes in the wind direction can cause the static inlet to miss the emission plume, leading to fluctuations in the measured real-time data (Fig. S2†). Some changes in the properties of the emitted plume were also observed with changing combustion regimes, with efficient flaming combustion during initial periods and inefficient smouldering combustion towards the last few minutes of the burns, which were associated with relatively larger concentrations of CO (Fig. S2†). Here, we use averages of the real-time measurements for every experiment for further calculations, to account for the whole burn cycle and facilitate comparison with the filter-derived measurements. The measured properties during the burns and ambient periods are summarised in Table S1.†

Table 1 Emission factors (g kg_{fuel}^{-1}) measured from the present study. The uncertainties reported here are the standard deviations around the mean values. We recommend using the standard deviation values or a relative standard deviation of 25%, whichever is greater, as the uncertainty of the reported emission factors

Pollutant	Straw	Stalks	Stems & leaves
N	4[a]	9[b]	3
CO_2	1306 ± 50	1343 ± 67	1389 ± 194
CO	97 ± 32	74 ± 43	86 ± 98
$PM_{2.5}$	7.5 ± 4.9	4.6 ± 2.2	19.3 ± 27.7
OC	2.1 ± 0.8	1.1 ± 0.9	7.6 ± 12.7
EC	1.9 ± 1.0	2.1 ± 1.0	0.9 ± 0.1
Ionic species (mg kg^{-1})[c]			
K^+	2383 ± 419	642 ± 457	468 ± 1150
Na^+	680 ± 203	184 ± 162	339 ± 101
NH_4^+	357 ± 80	56.7 ± 34.9	ND
SO_4^{2-}	178 ± 43	102 ± 65	44.1 ± 162.1
Mg^{2+}	ND	ND	9.67 ± 23.7
Cl^-	5923 ± 570	1761 ± 1015	10 509 ± 4996
Fl^-	ND	ND	11.3 ± 29.4
Br^-	ND	ND	3.61 ± 13.25
NO_3^-	ND	8.68 ± 1.32	ND
Elemental species (mg kg^{-1})[c]			
Al	443 ± 109	270 ± 132	1696 ± 469
Si	396 ± 117	311 ± 186	1603 ± 461
Ti	2.39 ± 1.31	2.89 ± 1.34	20.1 ± 10.5
V	0.51 ± 0.12	0.44 ± 0.24	3.91 ± 1.65
Mn	1.25 ± 0.87	1.49 ± 0.74	3.48 ± 1.09
Fe	17.5 ± 9.4	20.5 ± 10.3	99.7 ± 46.9
Cu	1.21 ± 1.54	9.18 ± 9.59	ND
As	1.84 ± 0.79	1.52 ± 0.81	16.0 ± 8.7
Se	0.06 ± 0.07	0.17 ± 0.07	0.3 ± 0.14
Rb	0.7 ± 0.85	1.31 ± 0.55	ND
Zr	1.89 ± 1.05	1.79 ± 0.83	18.0 ± 9.3
Mo	2.02 ± 0.82	2.1 ± 0.8	21.0 ± 10.8
Ba	1.15	0.5 ± 0.24	ND
Bi	4.35 ± 2.7	4.01 ± 1.74	31.9 ± 15.8
Hg	0.86 ± 0.55	0.82 ± 0.35	6.81 ± 3.47

[a] Totally four experiments were conducted but only three had complete speciation. [b] Nine experiments were conducted but experiments 1 and 2 were on the same filter and 3 and 4 were on the same filter. [c] Li^+, Ca^{2+}, NO_2^-, PO_4^{3-}, Sc, Cr, Zn, Ga, Sr, Cd, Sn, Sb, I, Cs, and Pb were not detected.

Filter-based measurements, conducted for the entire burn (including the ignition, flaming, and smouldering periods), were used to estimate the concentrations of $PM_{2.5}$ and its constituents. $PM_{2.5}$ elevations (up to 530 times the ambient) were used to calculate emission factors ranging from 4.6–19.3 g kg^{-1} (Fig. 2). $PM_{2.5}$ emission factors of straws (7.5 ± 4.9 g kg^{-1}) and stalks (4.6 ± 2.2 g kg^{-1}) were smaller than those for banana residue burns (19.3 ± 27.7 g kg^{-1}, discussed in more detail later). The dominant $PM_{2.5}$ chemical constituents were OC (8–40%) and EC (11–58%). The EC1 thermal carbon fraction expectedly dominates total EC (Fig. 2) and is sometimes referred to as char-EC and employed for biomass burning source

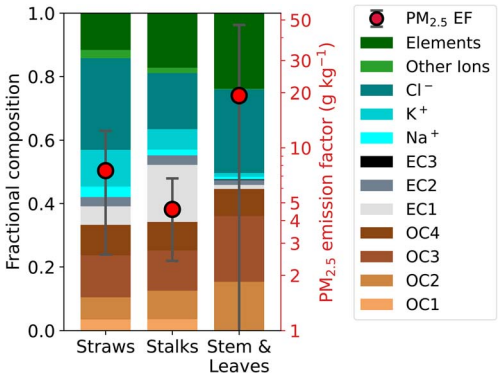

Fig. 2 Estimated emission factors of $PM_{2.5}$ from burning of different types of crop residues; red dots are mean values with error bars showing standard deviations (right *y*-axis, log-scale). The stacked-bar plots show the fractional contribution (left *y*-axis) of different chemical species, including organic carbon, black carbon, and other inorganic elements and ions. The elements are represented in their oxidised forms, and the organic carbon as organic matter using recommended factors from the literature.[91]

identification.[87,88] The OC/EC ratios in the emission plumes are close to 1 (range: 0.3–1.5) for stalks and straws, which are lower than previously reported ranges of 1.8–56.[32,33,38,39,89] These are also lower than the background values (11.75 ± 8.18). Similarly, the OC_{HV}/OC_{LV} ratio reduced from 1.43 ± 0.95 in the background to 0.48–0.68 during cereal and stalk residue burning measurements, indicating the dominance of lower volatility organic carbon particles in primary combustion emissions, which are shown to have strong absorption and longer atmospheric persistence.[51,90]

Emission factors were estimated for various other inorganic species (Table 1) to provide complete chemical speciation of the emissions (Fig. S3†), crucial for source apportionment studies. Amongst the inorganic species, Cl^- (9–47%) and K^+ (0–17%) are the most significant contributors to $PM_{2.5}$. Other species include Na^+, NH_4^+, SO_4^-, Al, and Si, with the remaining elements and ion emission factors in relative trace amounts (Table 1). We note that the emission factors of the inorganic species are crop-dependent, as opposed to carbonaceous aerosol emissions that are strongly dependent on the combustion conditions.[48,71,92] This crop-specificity of inorganic emission factors is evident in the above-detection-limit concentrations of certain species from emissions of specific residues, including NO_3^- from stalks and Fl^- and Br^- stems and leaves; these species were not detected from emissions of other residues. The emissions of inorganic species are likely influenced by the elemental composition of the residues, which are reported to vary with crop residues;[93] this will need to be substantiated in future emissions measurements.

The measured modified combustion efficiency (MCE) also affects the chemical composition. Emission factors from banana residues are larger for $PM_{2.5}$ (19.3 ± 27.7 g kg^{-1}) and OC (7.6 ± 12.7 g kg^{-1}), which are associated with lower combustion efficiencies (0.81 ± 0.12). Banana residues comprise leaves and pseudo-stems. The pseudo-stem carries much water that is retained for extended periods post-harvest. The composition of banana residues used in the experiments varies depending on the time from harvest. Burns conducted shortly after harvest have a higher proportion of leaves, which dry out faster. Conversely, burns performed later after harvest contain a greater proportion of stems, which have lower combustion efficiency due to their higher moisture content. In this study, measurements were made during both seasons. For this reason, we see large uncertainties (standard deviation) in measured emission factors from banana residue burning, with smaller emission factors from drier residue burns and larger factors measured when moist residues were burned. Since drier residue burns are more frequent, we report weighted average values of emission factors (more details in ESI Section S3†). Previous studies have also reported increased PM emission factors with increasing fuel moisture content.[39–41] In comparison, residues of straws and stalks are burned when dry and have higher combustion efficiencies of 0.89 ± 0.03 and 0.92 ± 0.05, respectively. These combustion efficiencies and subsequently emitted carbonaceous particles likely influence aerosol optical properties.

3.2 Relationships between aerosol chemical and optical properties

Intrinsic aerosol optical properties, the $AAE_{370/660}$ ($AAE_{660/880}$; $AAE_{370/880}$) and SSA_{532}, ranged from 0.89–3.8 (1.01–2; 0.94–3.21) and 0.29–0.83, respectively (Tables S1 and S2†). Previous field emission measurements from agricultural residue burning have reported AAEs: Stockwell *et al.*[37] measured an $AAE_{405/870}$ of 1.58–3.53 and Holder *et al.*[39] measured an $AAE_{405/871}$ of 1.6–3.1. Stockwell *et al.*[37] measured SSA_{405} ranging from 0.573–0.981, and Holder *et al.*[39] measured SSA_{532} ranging from 0.67–0.96. The AAEs and SSA measured in the present study are within the range of previous measurements but towards the lower end of the previously reported ranges (Table S2†).

Previous studies have shown that the modified combustion efficiency (MCE) can influence the relative emissions of OC and EC,[48,68,71] with larger OC emissions during smouldering (low MCE) and larger EC emissions during flaming (high MCE) combustion. These relative abundances can influence the optical properties of aerosol particles since EC particles have stronger absorption strengths (with smaller absorption dependence on the wavelength, or AAE) when compared to OC, which exhibits relatively weaker absorption (and larger AAEs). In the present study, we observe larger AAEs in fires with smaller MCE, and the two have a significant inverse correlation ($p < 0.1$, Fig. 3). Spearman-rank correlation coefficients are shown in Fig. 3 and discussed throughout this section, with significant correlations ($p < 0.1$) noted. The MCE correlates positively with absorption strength (MAC_{520}) and positively (significant) with the EC/PM ratio. The positive correlation between EC/PM and MAC_{520} is intuitive, as EC particles are stronger absorbers, and the overall aerosol mixture is likely absorbing with a larger contribution of EC to total PM. The OA (organic aerosol): EC ratios are also negatively correlated (significant) with MAC_{520} and positively with $AAE_{370/660}$. The combustion efficiency is also

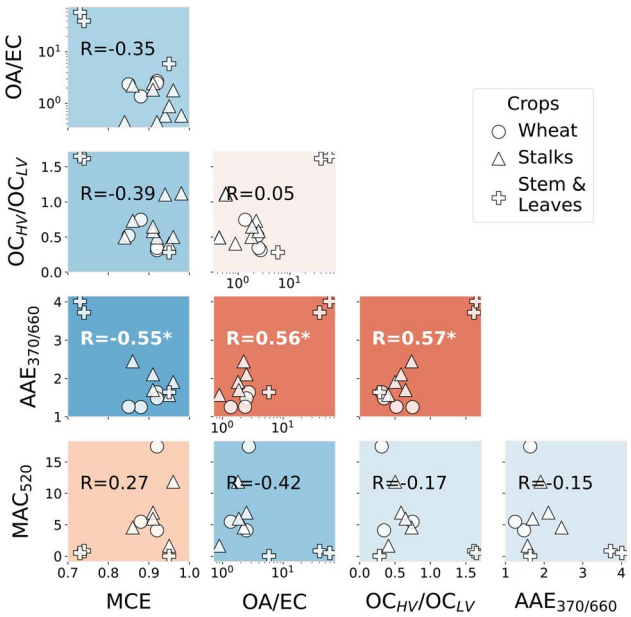

Fig. 3 Relationships between the modified combustion efficiency (MCE) and chemical (OA/EC and OC_{HV}/OC_{LV}) and optical properties ($AAE_{370/660}$ and MAC_{520}, in $m^2\ g^{-1}$) of aerosol particles emitted from crop residue burning. Each marker in the scatter plots represents an experiment. The numbers indicate non-parametric Spearman's rank correlation coefficients, and stars indicate significant correlations ($p < 0.1$). The colours of each sub-plot represent the strength of correlation (R), ranging from strong positive in dark red to weak correlations in white to strong negative correlations in dark blue.

negatively correlated with OC_{HV}/OC_{LV}, a ratio between the higher and lower volatility organic carbon fractions. Saleh *et al.*[46] proposed that as the combustion is more complete (*i.e.* higher combustion efficiency), more organic carbon particles reach lower volatility and optical behaviour closer to that of black carbon, *i.e.* long-chain graphite-like structures. These black-carbon-like particles have stronger absorption with weaker wavelength dependence of absorption and form a part of a continuum of absorption between weakly absorbing brown and strongly absorbing black carbon particles. This absorption continuum is also evident in the present study, as the $AAE_{370/660}$ positively correlates (significant), while MAC_{520} negatively correlates with OC_{HV}/OC_{LV}.

Carbonaceous aerosol absorption strength (MAC) is inversely correlated with absorption wavelength dependence (AAE), which was also previously reported.[47,94] The correlation is weak for the agricultural residue burning emissions measured in the present study; however, it follows an exponentially decaying pattern proposed by Cheng *et al.*[47] EC/PM is also correlated with the aerosol MAC, as also shown by Habib *et al.*[94] Previous studies[47,95] have also demonstrated the OC/EC ratio as positively and negatively correlated with AAE and MAC, which is also seen in the present study (Fig. S4†). Meanwhile, McClure *et al.*[48] showed a positive correlation between the MAC_{EC} (b_{abs}/EC) and OA/EC, as observed in the present study (Fig. S4†). The positive correlation between MAC_{EC} and OA/EC may be from additional absorption by brown (organic) carbon particles or enhancement in the absorption by black carbon particles because of non-absorbing coatings[49,96] (*via* the "lensing effect"[97]). Brown carbon particles may also contribute to mid-visible and near-IR absorption,[51] artificially enhancing MAC_{EC} values in the mid-visible wavelengths. The relationships presented here, despite not all being significant, provide new insight into the interrelationships between chemical, optical, and combustion properties of real-world biomass burning emissions, which agree with previous literature reporting emissions from other sources in controlled laboratory environments.

We do not explore more elaborate mathematical relationships between these properties due to the limited number of data points. We leave this exercise for another study that includes emission measurements from other biomass-burning emissions measured as a part of the COALESCE network emission measurements.[98] Here, we discuss the consistency of our measurements with relationships reported in previous lab-based studies studying aerosol emissions from various biomass fuel combustion sources.[48,70,71] These studies have proposed empirical equations using combustion efficiency (MCE), EC/OC, and OA/EC to estimate the AAE, SSA, and MAC_{EC}. The equations were developed by burning various biomass fuels that produce wide-ranging combustion conditions and chemical and optical properties. We used these equations for the range of chemical properties measured in the present study (of MCE, EC/OC, and OA/EC) to calculate optical properties; the empirical equation calculated values are compared to the measured values and summarised in Table S2.† Equations that use MCE to estimate AAEs[48,71] predict slightly higher values than the values measured in the present study ($AAE_{370/660} = 1.25–4.01$). However, the same studies recommend empirical equations using EC/OC[71] and OA/EC[48] that predict the AAE ranges in the present study more accurately. A similar behaviour is observed for equations calculating the SSA (observed $SSA_{532} = 0.29–0.83$) using EC/OC[71] and OA/EC,[48] which predict more accurately than equations using MCE.[48,70,71] Meanwhile, the MAC predicted by equations using EC/OC[47] and OA/EC[48] have much narrower ranges that do not predict the extremely low and high values measured in the present study ($MAC_{532,EC} = 0.33–44\ m^2\ g^{-1}$; $MAC_{532,PM} = 0.03–29\ m^2\ g^{-1}$). In summary, the parameters measured in the present study are within ranges of previous biomass combustion measurements but at the strongly absorbing end of the aerosol emissions measured on-field. The emission factors, when compared to the absorbing nature of the emitted aerosols, also reflect the absorbing nature of the emitted aerosols, as discussed in the next section.

3.3 Emission factors: comparison with previous studies

Global emission inventories typically use emission factors averaged from measurements across all crop types. The crop-invariant emission factors can lead to uncertainties in estimated emissions[63–65] and prompt the need to segregate emission factors for different crop residue types. Here, previously reported measurements were parsed from different crop types classified as straws (wheat, rice, maize, and barley)[33,34,36–39,41] and stalks (oilseeds and sugarcane).[34,37,99,100] The range of the literature reported factors is shown in the shaded areas in Fig. 4

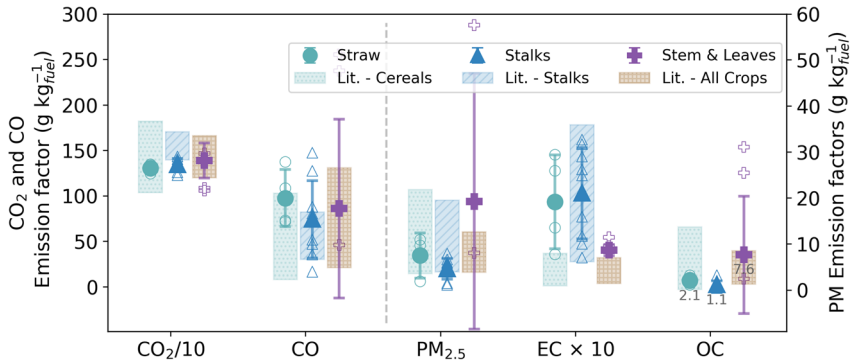

Fig. 4 Comparison between the measured emission factors and those reported by previous studies (shaded area). Factors for CO_2 and CO are on the left *y*-axis, and those for $PM_{2.5}$, EC, and OC are on the right *y*-axis. The open markers show individual measurements, and the filled markers show averaged values with error bars showing standard deviations. The shaded areas represent ranges of emission factors reported in previous studies for straw (green; wheat, rice, maize, and barley)[33,34,36–39,41] and stalks (blue; oilseeds and sugarcane),[34,37,99,100] and the brown shaded region shows the range (mean ± standard deviation) of emission factors used by global inventories.[15]

(green – straws, blue – stalks) along with those used by global inventories[65] ($\mu \pm \sigma$, as the yellow shaded area) to compare with the calculated emission factors in the present study. The emission factors of CO and CO_2 are within ranges of those reported in the literature and, consequently, the combustion efficiencies. The $PM_{2.5}$ (straw: 7.5 ± 4.9 g kg^{-1} and stalks: 4.6 ± 2.2 g kg^{-1}) and OC (straw: 2.1 ± 0.8 g kg^{-1} and stalks: 1.1 ± 0.9 g kg^{-1}) emission factors are within the ranges of previous measurements but at the lower end. Emission factors for stems and leaves residue burning are larger than those for other residue types and on the higher end of ranges reported by previous measurements. The EC emission factors for stalks (2.1 ± 1.0 g kg^{-1}) are within the ranges of earlier reports. However, EC emission factors for cereals (1.9 ± 1.0 g kg^{-1}) are larger than those reported previously for cereal crops and those used by global inventories. When compared to the emission factors used by global inventories[15] (Table S3†), the calculated emission factors of OC and $PM_{2.5}$ are towards the lower end of the reported range[65] (OC: 4.9 ± 3.6 g kg^{-1}, $PM_{2.5}$: 8.2 ± 4.4 g kg^{-1}), but that of EC is much higher—approximately 4–5 times the average value[65] (0.42 ± 0.28 g kg^{-1}). The larger emission factors of EC and relatively lower factors for OC are corroborated by the increased warming properties (larger MAC and lower SSA) of the emitted aerosols. The above evidence indicates the possibility of more flaming combustion conditions for straws in the region compared to other regions of the world. However, the EC emission factors for straws are similar to those reported for stalks in the present study and previous studies in other regions. Emission factors for non-absorbing aerosol species K^+ (0.4–2.4 g kg^{-1}) and Cl^- (1.7–10.6 g kg^{-1}) are within the range of previous estimates for K^+ (0.39–2.7 g kg^{-1}) but substantially larger for Cl^- (0.08–1.2 g kg^{-1}) when compared to previous lab[23,24,32] and field-measurements.[33] Next, we report the potential changes these emission factors have in the emission estimates.

3.4 Emissions from crop residue burning in India

Emissions from crop residue burning in India were estimated using the measured emission factors in the present study and the activity estimates from a previous study.[12] The emission factors of straws were used for all cereal crops (wheat, rice, maize, and millets), stalk factors for oilseeds, groundnut, cotton, and sugarcane, and leaves and stems factors for banana residue burning. In total, the emissions for the year 2019 of $PM_{2.5}$, OC, and EC were 567 Gg per year, 163 Gg per year, and 146 Gg per year, respectively. These emissions (of $PM_{2.5}$ and EC) are primarily from wheat (30% and 29%), rice (32% and 30%), and sugarcane (7% and 12%) residue burning (Fig. S5†). Over half of the OC emissions (from cereals) have low volatility (OC_{LV}), reported to exhibit strong absorption with longer absorption persistence.[46] The highest emitting states are Punjab, Uttar Pradesh, and Madhya Pradesh (Table S4†). The spatial variability is similar to that of the activity since the spatial variability in activity[12] is substantially larger than the variation of emission factors with crop types.

The emissions are calculated at high sub-national (district) and gridded (0.05° × 0.05°) scales to facilitate mitigation planning and climate modelling, respectively (Fig. 5a). Daily emissions estimates reveal that the emissions are primarily during the post-harvest periods corresponding to the rabi (March–May) and kharif (October–November) (Fig. 5b) seasons (see also additional ESI figures slideshow†). The emissions during the rabi harvest period are substantial and even larger than the kharif season emissions, especially for $PM_{2.5}$ (Fig. S6†) and OC (Fig. S7†). Significant rice residues are burned during the kharif post-harvest months in northwestern India, contributing to poor air-quality episodes in the region.[16,17] These poor air quality episodes have brought to the forefront the issue of crop residue burning and led to the misconception that crop residue burning is practised only in northwestern India. But in actuality, the burning of most other significant crop residues (wheat, sugarcane, and cotton) happens during other parts of the year (January–May). These emissions are larger but do not affect the air quality as much, probably because of more conducive ventilation conditions during the summer (post-rabi harvest) months.

We compare the updated emissions estimates with other regional and global emission inventories reporting emissions

from agricultural residue burning in India. Any differences in emission estimates are due to dissimilarities in activity and emission factors. Emissions, activity, and emission factors used by previous inventories, using bottom-up[13,66,101] and top-down[20] methods, are summarised in Table S3 and Fig. S8.† Bottom-up methods assume the fraction burned parameter[66,101] or estimate it using competing usage calculations,[66] whereas this study relies on activity data from country-wide surveys.[12] Previous inventories also used crop-averaged emission factors[20,66,101] or crop group averages for cereals and sugarcane.[13] We adopt an approach similar to that by Pandey *et al.*,[13] *i.e.*, crop group averaged emission factors for straws (cereals), stems (banana), and stalks (other crops). However, unlike previous studies that used emission factors measured in other world regions, we employ field-measured emission factors reported in the present study.

Compared to estimates from studies specifically reporting emissions over India, Pandey *et al.*[13] and Jain *et al.*,[66] there is a 39% and 27% decrease in the activity, respectively. There is a proportional decrease in the CO emissions (23–40%, since the emission factors are similar) but a substantial increase in the EC emissions (45–55%) because of a large increase in cereal emission factors in the present study. Meanwhile, OC emissions are 100–128% lower because of smaller measured emission factors. PM emissions are larger (32%) in comparison to those reported by Jain *et al.*[66] but smaller than those reported by Pandey *et al.*[13] When compared to the Emissions Database for Global Atmospheric Research (EDGAR_v6.1),[101] a global inventory using the bottom-up approach, there is a marginal decrease in the CO and PM emissions (<10%), but a large decrease in OC (61%) and increase in EC (167%) emissions. However, when compared to the Global Fire Emissions Database (GFED_4.1s),[20] using the top-down (satellite-based) approach, the present emissions are more than seven fold higher. The top-down method grossly underestimates the activity (8 fold lower), primarily because of the inability of satellite sensors to capture the small spatiotemporal resolution fires observed in India. In summary, there is a decrease in the emissions of PM and OC but an increase in the emissions of EC, which are likely to have implications for air quality and climate modelling efforts, especially for radiative forcing calculations.

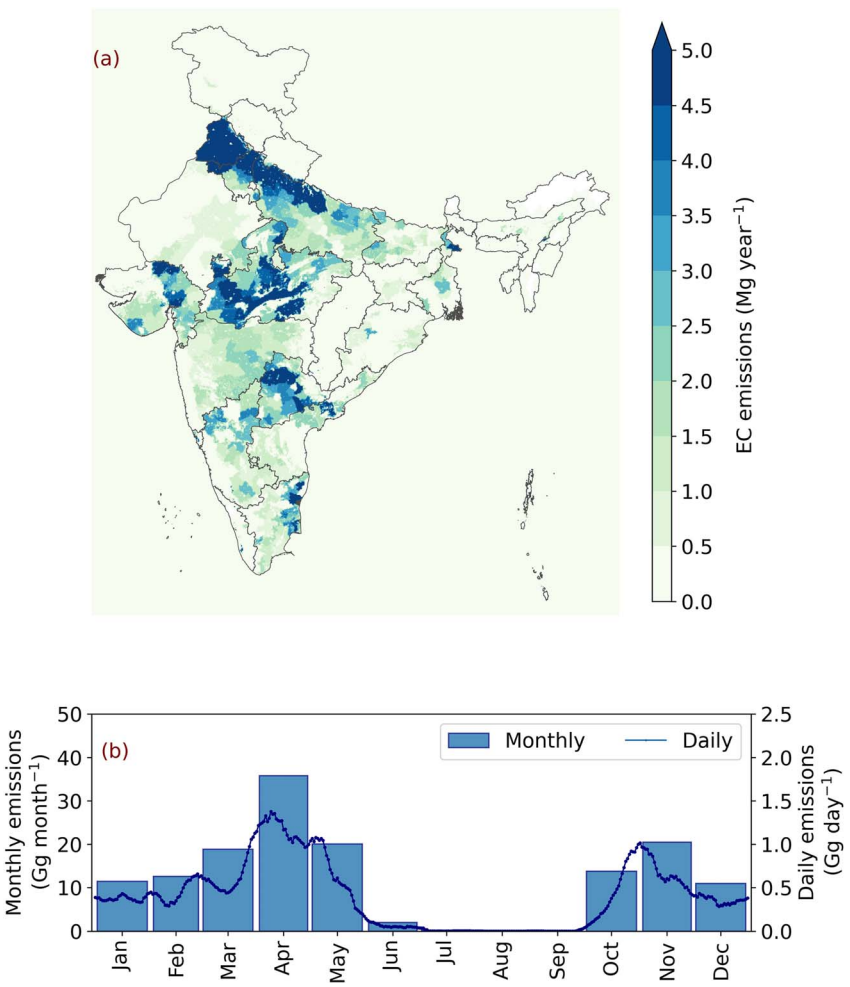

Fig. 5 (a) Gridded (0.05° × 0.05°) emissions of elemental carbon (Mg per year) from crop residue burning in India (b) monthly (Gg per month, left *y*-axis) and daily (Gg per day, right *y*-axis) variation of elemental carbon emissions across the year. Daily emissions are presented as 10-day running means for clarity.

3.5 Limitations

In this section, we discuss the limitations of the present study and the uncertainties that may arise from the limitations. With this section, we hope to apply additional context to the presented results and provide recommendations for future measurements of agricultural residue burning emissions in India and across the world. In the present study, we estimate emissions from crop residue burning across the country by assuming that the measurements made in western India represent the entire country. Burning practices (spread or piled on-field) are not expected to be different across the country,[12,42] however, variations in meteorological conditions may influence the emission properties. These are especially true for crops burned in different seasons. Most of the measurements presented in this study were made during the post-rabi (March–May) season, whereas some crops, most prominently rice, are burned during the post-kharif (October–November) burning season. This points to another limitation of the present study that emissions of not all the crops were measured. We divided the measured emission factors into three general categories, straws, stalks, and leaves and stems that most crop types should fit under. However, emission properties could differ for crops with very different biomass densities or elemental compositions of the residues. The burning of rice residue is likely to be similar to that of wheat residue burns, considering similar residue-to-crop ratios and spread-on-field configurations that both the crops are subjected to; however, further investigation is likely needed to verify this.

It may also be argued that the number of measurements for each crop type are not sufficient. While the number of measurements may be considered limited for general statistical significance, the experiment numbers are greater than or equal to the number of measurements of emission factors made by previous studies reporting emissions from this source. As also noted in the introduction, only two studies have reported emission factors for crop residue burning in the south-Asian region, which are limited by the number of measurements or crop types. Therefore, the emission factors presented are likely to be more accurate for emissions estimates than those derived from other world regions. Moreover, we report emission factors with uncertainty ranges arising from variability between experiments with the intention that they account for changes in emission factors because of changes in location and crop types observed across the country. Nevertheless, there remains room for improvement and additional measurements in future studies at other locations in the south-Asian region and of other crop types can aid in reducing the above uncertainties.

4 Conclusions

Open-field burning of agricultural waste is practised worldwide, contributing to warming carbonaceous aerosol emissions and poor air-quality episodes. However, there are limited field measurements with comprehensive chemical characterization and associated optical properties, which are crucial to estimating their climate impacts. This study reports chemical and optical properties of commonly field-burned crop residues in the south-Asian region, including residues from cotton and banana that are yet to be reported. The measurements reveal strongly absorbing aerosol emissions, as evidenced by the measured intrinsic aerosol optical properties (small AAEs, small SSAs, and large MACs). The emitted particles reveal properties near the strongly absorbing end of previous lab- and field-based biomass combustion emission measurements. These absorbing particles contain significant amounts of black carbon and lower volatility fractions of organic carbon, previously shown to be strongly absorbing in nature. There is an increase in the black carbon emission factors from crop residue burning relative to previously reported emission factors and, consequently, an increase in the total black carbon emissions. The emission factors reported here, along with recently reported activity estimates,[12] lead to a significant increase in EC emissions (83–167%), a moderate increase in CO (9–46%), and a substantial decrease in OC emissions (50–61%) compared to previous bottom-up estimates.[13,66,101] Together, the changes in CO (warming), OC (cooling), and EC (warming) can cause an overall increase in global warming potential of 1.64–3.84 times, relative to previous studies.[13,66,101] The above calculations use appropriate regional global warming potentials,[102] which consider organic carbon species as scattering only and not their absorbing nature. Including absorption by brown carbon particles, a subset of organic carbon, would further increase the warming potentials of the emissions from this source. These increased warming emissions can have implications for climate modelling estimates.

The recent Intergovernmental Panel on Climate Change's sixth assessment report shows that state-of-the-science climate modelling simulations underestimate the aerosol optical depth and absorption optical depth over the south-Asian region.[4,5] Focused regional studies also show an absorption underestimation.[61,103] These models use emission inventories that underestimate BC concentrations and do not consider the strongly absorbing BrC species emitted from crop residue burning. While some studies have shown BrC particles from smouldering fires to photo-bleach,[104–108] others have shown that lower volatility particles retain their absorptive nature for longer durations;[51,108,109] these lower volatility particles constitute ~63% of the total OC emissions in the present study. These BrC particles enhance total aerosol absorption when long-range transported biomass burning,[110] specifically crop waste burning emissions,[54,56,57,59,60,62] reach regional sites. Therefore, the insights from the present measurements and the updated, high spatiotemporal resolution emission estimates can aid in improving numerical weather, climate, and air-quality modelling simulations.[6,7,111]

Data availability

Data from the agricultural fire field emission measurements are available upon request (phuleria@iitb.ac.in).

Conflicts of interest

There are no conflicts to declare.

Acknowledgements

This work was supported by the Indian Ministry of Environment, Forest and Climate Change under the NCAP-COALESCE project grant no. 14/10/2014-CC(Vol. II). The authors thank the internal review committee of the NCAP-COALESCE project for their comments and suggestions on this paper. The views expressed in this document are solely those of the authors and do not necessarily reflect those of the Ministry. The Ministry does not endorse any products or commercial services mentioned in this publication. The authors thank all the farmers who allowed them to conduct field emission measurements for their patience and assistance. The authors also thank Ms Pradnya Lokhande for her assistance in preparing for the field measurements.

References

1 IPCC, *Global Warming of 1.5 °C*, Cambridge University Press, 2018.
2 D. Shindell, N. Borgford-Parnell, M. Brauer, A. Haines, J. C. Kuylenstierna, S. A. Leonard, V. Ramanathan, A. Ravishankara, M. Amann and L. Srivastava, A climate policy pathway for near- and long-term benefits, *Science*, 2017, **356**, 493–494.
3 K. Tibrewal and C. Venkataraman, Climate co-benefits of air quality and clean energy policy in India, *Nat. Sustain.*, 2021, **4**, 305–313.
4 J. Gliß, *et al.*, AeroCom phase III multi-model evaluation of the aerosol life cycle and optical properties using ground- and space-based remote sensing as well as surface in situ observations, *Atmos. Chem. Phys.*, 2021, **21**, 87–128.
5 S. Szopa, *et al.*, Short-Lived Climate Forcers, in *Climate Change 2021: The Physical Science Basis, Contribution of Working Group I to the Sixth Assessment Report of the Intergovernmental Panel on Climate Change*, 2022.
6 C. Venkataraman, *et al.*, Drivers of PM2.5 Episodes and Exceedance in India: A Synthesis From the COALESCE Network, *J. Geophys. Res.:Atmos.*, 2024, **129**, 1–18.
7 M. Sand, *et al.*, Aerosol absorption in global models from AeroCom phase III, *Atmos. Chem. Phys.*, 2021, **21**, 15929–15947.
8 C. Venkataraman, M. Bhushan, S. Dey, D. Ganguly, T. Gupta, G. Habib, A. Kesarkar, H. Phuleria and R. S. Raman, Indian network project on carbonaceous aerosol emissions, source apportionment and climate impacts (COALESCE), *Bull. Am. Meteorol. Soc.*, 2020, **101**, E1052–E1068.
9 G. Habib, *et al.*, Estimating shifts in fuel stacking among solid biomass fuels and liquified petroleum gas in rural households: a pan-India analysis, *Res. Sq.*, 2023, 1–18.
10 C. Navinya, *et al.*, Heating and lighting: understanding overlooked energy-consumption activities in the Indian residential sector, *Environ. Res. Commun.*, 2023, **5**, 045004.
11 K. Tibrewal, *et al.*, Reconciliation of energy use disparities in brick production in India, *Nat. Sustain.*, 2023, **6**, 1248–1257.
12 T. S. Kapoor, *et al.*, Reassessing the availability of crop residue as a bioenergy resource in India: a field-survey based study, *J. Environ. Manage.*, 2023, **341**, 118055.
13 A. Pandey, P. Sadavarte, A. V. Rao and C. Venkataraman, A technology-linked multi-pollutant inventory of Indian energy-use emissions: II. Residential, agricultural and informal industry sectors, *Atmos. Environ.*, 2014, **99**, 341–352.
14 T. C. Bond, D. G. Streets, K. F. Yarber, S. M. Nelson, J. H. Woo and Z. Klimont, A technology-based global inventory of black and organic carbon emissions from combustion, *J. Geophys. Res., D: Atmos.*, 2004, **109**, 1–43.
15 M. Andreae, Emission of trace gases and aerosols from biomass burning. Global biogeochemical, *Atmos. Chem. Phys.*, 2019, **15**(4), 955–966.
16 T. Mukherjee, A. Asutosh, S. K. Pandey, L. Yang, P. P. Gogoi, A. Panwar and V. Vinoj, Increasing potential for air pollution over megacity New Delhi: a study based on 2016 diwali episode, *Aerosol Air Qual. Res.*, 2018, **18**, 2510–2518.
17 H. Jethva, D. Chand, O. Torres, P. Gupta, A. Lyapustin and F. Patadia, Agricultural burning and air quality over northern india: a synergistic analysis using nasa's a-train satellite data and ground measurements, *Aerosol Air Qual. Res.*, 2018, **18**, 1756–1773.
18 P. Maheshwarkar, *et al.*, Understanding the Influence of Meteorology and Emission Sources on PM2.5 Mass Concentrations Across India: First Results From the COALESCE Network, *J. Geophys. Res.:Atmos.*, 2022, **127**, 1–15.
19 C. Wiedinmyer, S. K. Akagi, R. J. Yokelson, L. K. Emmons, J. A. Al-Saadi, J. J. Orlando and A. J. Soja, The Fire INventory from NCAR (FINN): a high resolution global model to estimate the emissions from open burning, *Geosci. Model Dev.*, 2011, **4**, 625–641.
20 G. R. V. D. Werf, J. T. Randerson, L. Giglio, T. T. V. Leeuwen, Y. Chen, B. M. Rogers, M. Mu, M. J. V. Marle, D. C. Morton, G. J. Collatz, R. J. Yokelson and P. S. Kasibhatla, Global fire emissions estimates during 1997-2016, *Earth Syst. Sci. Data*, 2017, **9**, 697–720.
21 IPCC, *2006 IPCC Guidelines for National Greenhouse Gas Inventories Volume 4 Agriculture, Forestry and Other Land Use*, 2006, vol. 94.
22 C. Venkataraman, G. Habib, D. Kadamba, M. Shrivastava, J. F. Leon, B. Crouzille, O. Boucher and D. G. Streets, Emissions from open biomass burning in India: integrating the inventory approach with high-resolution Moderate Resolution Imaging Spectroradiometer (MODIS) active-fire and land cover data, *Global Biogeochem. Cycles*, 2006, **20**, 1–12.
23 S. Turn, B. Jenkins, J. Chow, L. Pritchett, D. Campbell, T. Cahill and S. A. Whalen, Elemental characterization of particulate matter emitted from biomass burning: wind tunnel derived source profiles for herbaceous and wood fuels, *J. Geophys. Res.*, 1997, **102**, 3683–3699.
24 M. D. Hays, P. M. Fine, C. D. Geron, M. J. Kleeman and B. K. Gullett, Open burning of agricultural biomass:

physical and chemical properties of particle-phase emissions, *Atmos. Environ.*, 2005, **39**, 6747–6764.

25 R. Dhammapala, C. Claiborn, C. Simpson and J. Jimenez, Emission factors from wheat and Kentucky bluegrass stubble burning: comparison of field and simulated burn experiments, *Atmos. Environ.*, 2007, **41**, 1512–1520.

26 H. Zhang, X. Ye, T. Cheng, J. Chen, X. Yang, L. Wang and R. Zhang, A laboratory study of agricultural crop residue combustion in China: emission factors and emission inventory, *Atmos. Environ.*, 2008, **42**, 8432–8441.

27 H. Ni, Y. Han, J. Cao, L. W. Chen, J. Tian, X. Wang, J. C. Chow, J. G. Watson, Q. Wang, P. Wang, H. Li and R. J. Huang, Emission characteristics of carbonaceous particles and trace gases from open burning of crop residues in China, *Atmos. Environ.*, 2015, **123**, 399–406.

28 J. Tian, J. C. Chow, J. Cao, Y. Han, H. Ni, L. W. A. Chen, X. Wang, R. Huang, H. Moosmüller and J. G. Watson, A biomass combustion chamber: design, evaluation, and a case study of wheat straw combustion emission tests, *Aerosol Air Qual. Res.*, 2015, **15**, 2104–2114.

29 C. Li, Y. Hu, F. Zhang, J. Chen, Z. Ma, X. Ye, X. Yang, L. Wang, X. Tang, R. Zhang, M. Mu, G. Wang, H. Kan, X. Wang and A. Mellouki, Multi-pollutant emissions from the burning of major agricultural residues in China and the related health-economic effects, *Atmos. Chem. Phys.*, 2017, **17**, 4957–4988.

30 Z. Fang, *et al.*, Open burning of rice, corn and wheat straws: primary emissions, photochemical aging, and secondary organic aerosol formation, *Atmos. Chem. Phys.*, 2017, **17**, 14821–14839.

31 Y. Zhang, M. Shao, Y. Lin, S. Luan, N. Mao, W. Chen and M. Wang, Emission inventory of carbonaceous pollutants from biomass burning in the Pearl River Delta Region, China, *Atmos. Environ.*, 2013, **76**, 189–199.

32 X. Li, S. Wang, L. Duan, J. Hao, C. Li, Y. Chen and L. Yang, Particulate and trace gas emissions from open burning of wheat straw and corn stover in China, *Environ. Sci. Technol.*, 2007, **41**, 6052–6058.

33 N. T. K. Oanh, B. T. Ly, D. Tipayarom, B. R. Manandhar, P. Prapat, C. D. Simpson and L. J. S. Liu, Characterization of particulate matter emission from open burning of rice straw, *Atmos. Environ.*, 2011, **45**, 493–502.

34 T. Zhang, M. J. Wooster, D. C. Green and B. Main, New field-based agricultural biomass burning trace gas, PM2.5, and black carbon emission ratios and factors measured in situ at crop residue fires in Eastern China, *Atmos. Environ.*, 2014, **121**, 22–34.

35 S. Kudo, H. Tanimoto, S. Inomata, S. Saito, X. Pan, Y. Kanaya, F. Taketani, Z. Wang, H. Chen, H. Dong, M. Zhang and K. Yamaji, Emissions of nonmethane volatile organic compounds from open crop residue burning in the Yangtze River Delta region, China, *J. Geophys. Res.:Atmos.*, 2014, **119**, 7684–7698.

36 N. T. K. Oanh, A. Tipayarom, T. L. Bich, D. Tipayarom, C. D. Simpson, D. Hardie and L. J. S. Liu, Characterization of gaseous and semi-volatile organic compounds emitted from field burning of rice straw, *Atmos. Environ.*, 2015, **119**, 182–191.

37 C. E. Stockwell, T. J. Christian, J. D. Goetz, T. Jayarathne, P. V. Bhave, P. S. Praveen, S. Adhikari, R. Maharjan, P. F. DeCarlo, E. A. Stone, E. Saikawa, D. R. Blake, I. J. Simpson, R. J. Yokelson and A. K. Panday, Nepal Ambient Monitoring and Source Testing Experiment (NAMaSTE): emissions of trace gases and light-absorbing carbon from wood and dung cooking fires, garbage and crop residue burning, brick kilns, and other sources, *Atmos. Chem. Phys.*, 2016, **16**, 11043–11081.

38 S. Sahai, C. Sharma, D. P. Singh, C. K. Dixit, N. Singh, P. Sharma, K. Singh, S. Bhatt, S. Ghude, V. Gupta, R. K. Gupta, M. K. Tiwari, S. C. Garg, A. P. Mitra and P. K. Gupta, A study for development of emission factors for trace gases and carbonaceous particulate species from in situ burning of wheat straw in agricultural fields in India, *Atmos. Environ.*, 2007, **41**, 9173–9186.

39 A. L. Holder, B. K. Gullett, S. P. Urbanski, R. Elleman, S. O'Neill, D. Tabor, W. Mitchell and K. R. Baker, Emissions from prescribed burning of agricultural fields in the Pacific Northwest, *Atmos. Environ.*, 2017, **166**, 22–33.

40 R. K. Chakrabarty, M. Gyawali, R. L. Yatavelli, A. Pandey, A. C. Watts, J. Knue, L. W. A. Chen, R. R. Pattison, A. Tsibart, V. Samburova and H. Moosmüller, Brown carbon aerosols from burning of boreal peatlands: microphysical properties, emission factors, and implications for direct radiative forcing, *Atmos. Chem. Phys.*, 2016, **16**, 3033–3040.

41 B. C. Nguyen, J. P. Putaud, N. Mihalopoulos, B. Bonsang and C. Doan, CH4 and CO emissions from rice straw burning in South East Asia, *Environ. Monit. Assess.*, 1994, **31–31**, 131–137.

42 IARI, *Crop Residues Management with Conservation Agriculture: Potential, Constraints and Policy Needs*, Indian Agricultural Research Institute, 2012, vol. vii, p. 32.

43 T. C. Bond, *et al.*, Bounding the role of black carbon in the climate system: a scientific assessment, *J. Geophys. Res.:Atmos.*, 2013, **118**, 5380–5552.

44 M. O. Andreae and A. Gelencsér, Black carbon or brown carbon? the nature of light-absorbing carbonaceous aerosols, *Atmos. Chem. Phys.*, 2006, **6**, 3131–3148.

45 A. Laskin, J. Laskin and S. A. Nizkorodov, Chemistry of Atmospheric Brown Carbon, *Chem. Rev.*, 2015, **2015**, 4335–4382.

46 R. Saleh, Z. Cheng and K. Atwi, The Brown–Black Continuum of Light-Absorbing Combustion Aerosols, *Environ. Sci. Technol. Lett.*, 2018, **5**, 508–513.

47 Z. Cheng, K. Atwi, T. Onyima and R. Saleh, Investigating the dependence of light-absorption properties of combustion carbonaceous aerosols on combustion conditions, *Aerosol Sci. Technol.*, 2019, **53**, 419–434.

48 C. D. McClure, C. Y. Lim, D. H. Hagan, J. H. Kroll and C. D. Cappa, Biomass-burning-derived particles from a wide variety of fuels - Part 1: properties of primary particles, *Atmos. Chem. Phys.*, 2020, **20**, 1531–1547.

49 Z. Fang, W. Deng, X. Wang, Q. He, Y. Zhang, W. Hu, W. Song, M. Zhu, S. Lowther, Z. Wang, X. Fu, Q. Hu, X. Bi, C. George and Y. Rudich, Evolution of light absorption properties during photochemical aging of straw open burning aerosols, *Sci. Total Environ.*, 2022, **838**, 156431.
50 G. Adler, N. L. Wagner, K. D. Lamb, K. M. Manfred, J. P. Schwarz, A. Franchin, A. M. Middlebrook, R. A. Washenfelder, C. C. Womack, R. J. Yokelson and D. M. Murphy, Evidence in biomass burning smoke for a light-absorbing aerosol with properties intermediate between brown and black carbon, *Aerosol Sci. Technol.*, 2019, **53**, 976–989.
51 R. K. Chakrabarty, *et al.*, Shortwave absorption by wildfire smoke dominated by dark brown carbon, *Nat. Geosci.*, 2023, **16**, 683–688.
52 D. T. L. Alexander, P. A. Crozier and J. R. Anderson, Brown Carbon Spheres in East Asian Outflow and Their Optical Properties, *Science*, 2008, **321**, 833–836.
53 J. C. Corbin, *et al.*, Infrared-absorbing carbonaceous tar can dominate light absorption by marine-engine exhaust, *npj Clim. Atmos. Sci.*, 2019, **2**, 1–10.
54 T. S. Kapoor, C. Venkataraman, C. Sarkar, H. C. Phuleria, A. Chatterjee, G. Habib and J. S. Apte, Estimation of real-time brown carbon absorption: an observationally constrained Mie theory-based optimization method, *J. Aerosol Sci.*, 2022, **166**, 106047.
55 S. Bikkina and M. Sarin, Brown carbon in the continental outflow to the North Indian Ocean, *Environ. Sci.: Processes Impacts*, 2019, **21**, 970–987.
56 B. Srinivas, N. Rastogi, M. Sarin, A. Singh and D. Singh, Mass absorption efficiency of light absorbing organic aerosols from source region of paddy-residue burning emissions in the Indo-Gangetic Plain, *Atmos. Environ.*, 2016, **125**, 360–370.
57 R. Satish, N. Rastogi, A. Singh and D. Singh, Change in characteristics of water-soluble and water-insoluble brown carbon aerosols during a large-scale biomass burning, *Environ. Sci. Pollut. Res.*, 2020, **27**, 33339–33350.
58 M. Devaprasad, N. Rastogi, R. Satish, A. Patel, A. Singh, A. Dabhi, A. Shivam, R. Bhushan and R. Meena, Characterization of paddy-residue burning derived carbonaceous aerosols using dual carbon isotopes, *Sci. Total Environ.*, 2023, **864**, 161044.
59 V. Choudhary, G. K. Singh, T. Gupta and D. Paul, Absorption and radiative characteristics of brown carbon aerosols during crop residue burning in the source region of Indo-Gangetic Plain, *Atmos. Res.*, 2021, **249**, 105285.
60 A. Soni, A. Chatterjee, B. K. Saikia and T. Gupta, Mass and Light Absorption Properties of Atmospheric Carbonaceous Aerosols over the Outflow Regions of Indo-Gangetic Plain, *Atmos. Environ.*, 2024, **325**, 120413.
61 T. S. Kapoor, H. C. Phuleria, B. Sumlin, N. Shetty, G. Anurag, M. Bansal, S. S. Duhan, M. S. Khan, J. S. Laura, P. Manwani, R. K. Chakrabarty and C. Venkataraman, Optical properties and refractive index of wintertime aerosol at a highly polluted north-Indian site, *J. Geophys. Res.:Atmos.*, 2023, e2022JD038272.
62 T. S. Kapoor, *et al.*, Spatial Distribution in Surface Aerosol Light Absorption Across India, *Geophys. Res. Lett.*, 2024, **51**, 1–13.
63 S. K. Akagi, R. J. Yokelson, C. Wiedinmyer, M. J. Alvarado, J. S. Reid, T. Karl, J. D. Crounse and P. O. Wennberg, Emission factors for open and domestic biomass burning for use in atmospheric models, *Atmos. Chem. Phys.*, 2011, **11**, 4039–4072.
64 M. O. Andreae and P. Merlet, Emission of trace gases and aerosols from biomass burning, *Global Biogeochem. Cycles*, 2001, **15**, 955–966.
65 M. O. Andreae, *Biomass Burning Emission Factors*, 2019.
66 N. Jain, A. Bhatia and H. Pathak, Emission of air pollutants from crop residue burning in India, *Aerosol Air Qual. Res.*, 2014, **14**, 422–430.
67 J. Kumari, M. S. Khan, M. Bansal, T. S. Kapoor and G. Habib, Design, Evaluation, and Performance of Versatile Source Sampling System (VS3) for Monitoring and Characterization of Aerosols from Area, Point and Line Sources, *Aerosol Sci. Technol.*, 2024, **58**(12), 1333–1346.
68 C. A. Roden, T. C. Bond, S. Conway and A. B. O. Pinel, Emission factors and real-time optical properties of particles emitted from traditional wood burning cookstoves, *Environ. Sci. Technol.*, 2006, **40**, 6750–6757.
69 J. Prakash, G. Habib and S. Kumar, Evaluation of portable dilution system for aerosol measurement from stationary and mobile combustion sources, *Aerosol Sci. Technol.*, 2016, **50**, 717–731.
70 S. Liu, A. C. Aiken, C. Arata, M. K. Dubey, C. E. Stockwell, R. J. Yokelson, E. A. Stone, T. Jayarathne, A. L. Robinson, P. J. DeMott and S. M. Kreidenweis, Aerosol single scattering albedo dependence on biomass combustion efficiency: laboratory and field studies, *Geophys. Res. Lett.*, 2014, **41**, 742–748.
71 R. P. Pokhrel, N. L. Wagner, J. M. Langridge, D. A. Lack, T. Jayarathne, E. A. Stone, C. E. Stockwell, R. J. Yokelson and S. M. Murphy, Parameterization of single-scattering albedo (SSA) and absorption Ångström exponent (AAE) with EC/OC for aerosol emissions from biomass burning, *Atmos. Chem. Phys.*, 2016, **16**, 9549–9561.
72 L. Drinovec, G. Močnik, P. Zotter, A. S. Prévôt, C. Ruckstuhl, E. Coz, M. Rupakheti, J. Sciare, T. Müller, A. Wiedensohler and A. D. Hansen, The "dual-spot" Aethalometer: an improved measurement of aerosol black carbon with real-time loading compensation, *Atmos. Meas. Tech.*, 2015, **8**, 1965–1979.
73 T. L. Anderson and J. A. Ogren, Determining Aerosol Radiative Properties Using the TSI 3563 Integrating Nephelometer, *Aerosol Sci. Technol.*, 1998, **29**, 57–69.
74 D. Haswani, R. S. Raman, K. Yadav, A. Dhandapani, J. Iqbal, R. N. Kumar, S. V. Laxmi Prasad, A. Yogesh, B. M. Sadashiva Murthy and K. S. Lokesh, Pollution characteristics and ecological risks of trace elements in PM2.5 over three COALESCE network sites – Bhopal, Mesra, and Mysuru, India, *Chemosphere*, 2023, **324**, 138203.

75 K. Yadav, R. S. Raman, A. Bhardwaj, D. Paul, T. Gupta, D. Shukla, S. L. Prasad, K. Lokesh and P. Venkatesh, Tracing the predominant sources of carbon in PM2.5 using delta-13C values together with OC/EC and select inorganic ions over two COALESCE locations, *Chemosphere*, 2022, **308**, 136420.
76 A. Bhardwaj and R. S. Raman, Evaluation of organic aerosol filter sampling artefacts and implications to gravimetric PM2.5 mass at a COALESCE network site – Bhopal, India, *J. Environ. Manage.*, 2022, **319**, 115749.
77 J. C. Chow, J. G. Watson, L. W. Chen, M. C. Chang, N. F. Robinson, D. Trimble and S. Kohl, The IMPROVE_A temperature protocol for thermal/optical carbon analysis: maintaining consistency with a long-term database, *J. Air Waste Manage. Assoc.*, 2007, **57**, 1014–1023.
78 J. Ma, X. Li, P. Gu, R. Timothy, A. A. P. Dallmann and N. M. Donahue, Estimating ambient particulate organic carbon concentrations and partitioning using thermal optical measurements and the volatility basis set, *Aerosol Sci. Technol.*, 2016, **50**, 638–651.
79 N. Shetty, P. Liu, Y. Liang, B. Sumlin, C. Daube, S. Herndon, A. H. Goldstein and R. K. Chakrabarty, Brown carbon absorptivity in fresh wildfire smoke: associations with volatility and chemical compound groups, *Environ. Sci.: Atmos.*, 2023, **3**, 1262–1271.
80 J. Zhang, K. R. Smith, Y. Ma, S. Ye, F. Jiang, W. Qi, P. Liu, M. A. Khalil, R. A. Rasmussen and S. A. Thorneloe, Greenhouse gases and other airborne pollutants from household stoves in China: a database for emission factors, *Atmos. Environ.*, 2000, **34**, 4537–4549.
81 MOAFW, *Crop Production Statistics Information System*, Directorate of Economics & Statistics, Ministry of Agriculture and Farmers Welfare, Govt. of India, 2008, **https://aps.dac.gov.in/APY/Index.htm**.
82 CGPL, *Biomass Atlas*, Combustion Gasification & Propulsion Laboratory, IISc, Bangalore, 2009, **https://lab.cgpl.iisc.ernet.in/atlas/SDA/cropimages.pdf**.
83 MHA, *Census of India*, Office of the Registrar General and Census Commissioner, India, 2011, **https://censusindia.gov.in/2011-common/censusdata2011.html**.
84 DAHD, *20th Livestock Census*, Department of Animal Husbandry and Dairying, Government of India, 2019.
85 L. Giglio, L. Boschetti, D. Roy, A. A. Hoffman, M. Humber and J. V. Hall, *Collection 6 MODIS Burned Area Product User Guide*, 2018.
86 D. Sulla-Menashe and M. A. Friedl, *User Guide to Collection 6 MODIS Land Cover (MCD12Q1 and MCD12C1) Product*, 2018, DOI: **10.5067/MODIS/MCD12Q1.006**.
87 Y. Han, J. Cao, J. C. Chow, J. G. Watson, Z. An, Z. Jin, K. Fung and S. Liu, Evaluation of the thermal/optical reflectance method for discrimination between char- and soot-EC, *Chemosphere*, 2007, **69**, 569–574.
88 Y. M. Han, J. Cao, S. C. Lee, K. F. Ho and Z. S. An, Different characteristics of char and soot in the atmosphere and their ratio as an indicator for source identification in Xi'an, China, *Atmos. Chem. Phys.*, 2010, **10**, 595–607.
89 T. Jayarathne, C. E. Stockwell, P. V. Bhave, P. S. Praveen, C. M. Rathnayake, R. M. Islam, A. K. Panday, S. Adhikari, R. Maharjan, J. D. Goetz, P. F. Decarlo, E. Saikawa, R. J. Yokelson and E. A. Stone, Nepal Ambient Monitoring and Source Testing Experiment (NAMaSTE): emissions of particulate matter from wood-and dung-fueled cooking fires, garbage and crop residue burning, brick kilns, and other sources, *Atmos. Chem. Phys.*, 2018, **18**, 2259–2286.
90 R. Saleh, From Measurements to Models: Toward Accurate Representation of Brown Carbon in Climate Calculations, *Curr. Pollut. Rep.*, 2020, **6**, 90–104.
91 J. C. Chow, D. H. Lowenthal, L.-W. A. Chen, X. Wang and J. G. Watson, Mass reconstruction methods for PM2.5: a review, *Air Qual., Atmos. Health*, 2015, **8**, 243–263.
92 R. Saleh, E. S. Robinson, D. S. Tkacik, A. T. Ahern, S. Liu, A. C. Aiken, R. C. Sullivan, A. A. Presto, M. K. Dubey, R. J. Yokelson, N. M. Donahue and A. L. Robinson, Brownness of organics in aerosols from biomass burning linked to their black carbon content, *Nat. Geosci.*, 2014, **7**, 647–650.
93 I. Obernberger, F. Biedermann, W. Widmann and R. Riedl, Concentrations of inorganic elements in biomass fuels and recovery in the different ash fractions, *Biomass Bioenergy*, 1997, **12**, 211–224.
94 G. Habib, C. Venkataraman, T. C. Bond and J. J. Schauer, Chemical, Microphysical and Optical Properties of Primary Particles from the Combustion of Biomass Fuels Chemical, Microphysical and Optical Properties of Primary Particles from the Combustion of Biomass Fuels, *Environ. Sci. Technol.*, 2008, 8829–8834.
95 R. P. Pokhrel, E. R. Beamesderfer, N. L. Wagner, J. M. Langridge, D. A. Lack, T. Jayarathne, E. A. Stone, C. E. Stockwell, R. J. Yokelson and S. M. Murphy, Relative importance of black carbon, brown carbon, and absorption enhancement from clear coatings in biomass burning emissions, *Atmos. Chem. Phys.*, 2017, **17**, 5063–5078.
96 P. Beeler and R. K. Chakrabarty, Constraining the particle-scale diversity of black carbon light absorption using a unified framework, *Atmos. Chem. Phys.*, 2022, **22**, 14825–14836.
97 K. A. Fuller, W. C. Malm and S. M. Kreidenweis, Effects of mixing on extinction by carbonaceous particles, *J. Geophys. Res.:Atmos.*, 1999, **104**, 15941–15954.
98 C. Navinya, T. S. Kapoor, G. Anurag, C. Venkataraman, H. C. Phuleria and R. K. Chakrabarty, Brownness of Organics in Anthropogenic Biomass Burning Aerosols over South Asia, *Atmos. Chem. Phys.*, 2024, **24**, 13285–13297.
99 M. O. Andreae, T. W. Andreae, H. Annegarn, J. Beer, H. Cachier, P. Canut, W. Elbert, W. Maenhaut, I. Salma, F. G. Wienhold, T. Zenker and M. Planck, Airborne Studies Africa: 2. Aerosol Chemical Composition, *J. Geophys. Res.*, 1998, **103**, 119–128.
100 R. Koppmann, A. Khedim, J. Rudolph, D. Poppe, M. O. Andreae, G. Helas, M. Welling and T. Zenker, Emissions of organic trace gases from savanna fires in southern Africa during the 1992 Southern African Fire

Atmosphere Research Initiative and their impact on the formation of tropospheric ozone, *J. Geophys. Res.:Atmos.*, 1997, **102**, 18879–18888.

101 F. M. Ferrario, M. Crippa, D. Guizzardi, M. Muntean, E. Schaaf, M. Banja, F. Pagani and E. Solazzo, *EDGAR v6.1 Global Air Pollutant Emissions*, European Commission, Joint Research Centre (JRC), 2022.

102 K. Tanaka, O. Cavalett, W. J. Collins and F. Cherubini, Asserting the climate benefits of the coal-to-gas shift across temporal and spatial scales, *Nat. Clim. Change*, 2019, **9**, 389–396.

103 T. Sarkar, S. Anand, A. Bhattacharya, A. Sharma, C. Venkataraman, A. Sharma, D. Ganguly and R. Bhawar, Evaluation of the simulated aerosol optical properties over India: COALESCE model inter-comparison of three GCMs with ground and satellite observations, *Sci. Total Environ.*, 2022, **852**, 158442.

104 B. J. Sumlin, A. Pandey, M. J. Walker, R. S. Pattison, B. J. Williams and R. K. Chakrabarty, Atmospheric Photooxidation Diminishes Light Absorption by Primary Brown Carbon Aerosol from Biomass Burning, *Environ. Sci. Technol. Lett.*, 2017, **4**, 540–545.

105 E. C. Browne, X. Zhang, J. P. Franklin, K. J. Ridley, T. W. Kirchstetter, K. R. Wilson, C. D. Cappa and J. H. Kroll, Effect of heterogeneous oxidative aging on light absorption by biomass burning organic aerosol, *Aerosol Sci. Technol.*, 2019, **53**, 663–674.

106 E. G. Schnitzler, N. G. Gerrebos, T. S. Carter, Y. Huang, C. L. Heald, A. K. Bertram and J. P. Abbatt, Rate of atmospheric brown carbon whitening governed by environmental conditions, *Proc. Natl. Acad. Sci. U. S. A.*, 2022, **119**, e2205610119.

107 M. Zhong and M. Jang, Dynamic light absorption of biomass-burning organic carbon photochemically aged under natural sunlight, *Atmos. Chem. Phys.*, 2014, **14**, 1517–1525.

108 J. P. S. Wong, A. Nenes and R. J. Weber, Changes in Light Absorptivity of Molecular Weight Separated Brown Carbon Due to Photolytic Aging, *Environ. Sci. Technol.*, 2017, **51**, 8414–8421.

109 A. K. Y. Lee, M. D. Willis, R. M. Healy, J. M. Wang, C.-H. Jeong, J. C. Wenger, G. J. Evans and J. P. D. Abbatt, Single-particle characterization of biomass burning organic aerosol (BBOA): evidence for non-uniform mixing of high molecular weight organics and potassium, *Atmos. Chem. Phys.*, 2016, **16**, 5561–5572.

110 Q. Wang, Y. Han, J. Ye, S. Liu, S. Pongpiachan, N. Zhang, Y. Han, J. Tian, C. Wu, X. Long, Q. Zhang, W. Zhang, Z. Zhao and J. Cao, High Contribution of Secondary Brown Carbon to Aerosol Light Absorption in the Southeastern Margin of Tibetan Plateau, *Geophys. Res. Lett.*, 2019, **46**, 4962–4970.

111 T. Sarkar, T. S. Kapoor, Y. Mayya, C. Venkataraman and S. Anand, Near-source dispersion and coagulation parameterization: application to biomass burning emissions, *Atmos. Environ.:X*, 2024, **22**, 100266.